Electron Transfer Complexes of the System Pyrene/PMDA Studied by Transient Absorption and Degenerate Four-Wave Mixing Measurements

M. Assel, T. Höfer, A. Laubereau,* and W. Kaiser

Physik Department E 11, Technische Universität München, D-85748 Garching, Germany

Received: February 15, 1996; In Final Form: May 21, 1996[⊗]

The kinetics of the intermolecular electron transfer between pyrene and pyromelitic dianhydride is studied by two experimental techniques: transient absorption measurements and degenerate four-wave mixing after optical excitation by picosecond light pulses. The observed time evolution of the electron transfer reaction depends strongly on the wavelength of the pump pulse. Excitation of pyrene leads to a diffusion-controlled electron transfer (in agreement with theoretical calculations), while excitation of the ground state donor−acceptor complex shows a different time behavior. Comparison of the decay times and the molecular hyperpolarizabilities provides clear evidence for two different excited charge transfer complexes.

1. Introduction

Several mixtures of aromatic molecules with acid anhydrides are known to undergo electron transfer upon photoexcitation. In some cases a complex is formed without optical excitation, which is called a ground state donor−acceptor complex (DAC).[1−4] Previous publications examining these charge transfer systems—dissolved in the polar solvent acetonitrile (ϵ = 37.4)—show a characteristic ground state DAC absorption band.[5] The investigations presented in the following are performed with solutions of the aromatic molecules pyrene (Py) and pyromelitic dianhydride (PMDA) in the solvent tetrahydrofurane (THF). The molecules form a DAC ground state

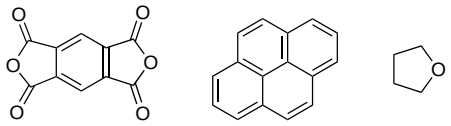

pyromelitic dianhydride pyrene tetrahydrofurane

complex described previously,[5] as indicated by the visible absorption spectrum (see Figure 1). A new, broad absorption band appears in the spectrum with a maximum position at $\tilde{\nu}$ = 21 600 cm^{-1}, which is attributed to the DAC. Photoexcitation at a frequency lying within this absorption band results in the appearance of two new transient absorption bands, one located at 452 nm, the other at 670 nm, which correspond to absorption bands of the cation of pyrene and the anion of PMDA, respectively.[6] This fact gives evidence that a charge transfer complex (CTI) is formed immediately after the excitation of the DAC. The decay of the transient absorption of these bands was found to be fast, the time constant depending strongly on the polarity of the solvent and ranging between ∼10 ps in acetonitrile (ϵ = 37.4) and 410 ps in benzene (ϵ = 2.3).[5] The short relaxation is explained by the fast charge recombination back to the ground state DAC.

According to these experiments, the following reaction scheme is suggested:

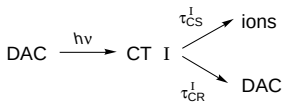

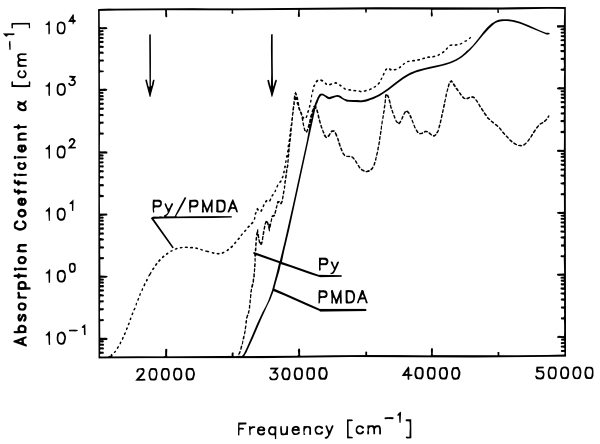

Figure 1. Measured absorption coefficient α versus frequency for pure pyrene (dashed line), pure PMDA (solid line), and the mixture of pyrene/PMDA dissolved in tetrahydrofurane, concentrations c_{Py} = 0.01 M and c_{PMDA} = 0.2 M. The arrows mark the frequency positions where the pyrene/PMDA solution is excited in pump−probe and DFWM experiments.

Besides the excitation at the DAC absorption band the donor molecule—here pyrene—of the electron transfer system may be directly excited. In polar solvents this excitation step also initiates an electron transfer process. Now the dynamics of the photoreaction is different from that which is observed after excitation of the DAC. The following reaction scheme may be assumed for the excitation of the donor molecule[5] (for comparison we point to a similar system like perylene/phthalic anhydride[4,7]).

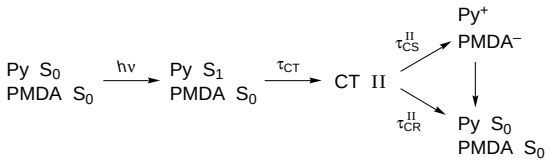

After exciting the ground state pyrene via the $S_0 \rightarrow S_1$ transition an electron is transferred by encounter between the excited pyrene and the ground state PMDA. This process is diffusion controlled, causing a rate constant that depends linearly on the concentration of the acceptor molecule PMDA.[8,9] In this way a new charge transfer complex (CTII) is formed. This complex can disintegrate in two different ways. One channel leads to the ground state of the two participating molecules by charge

[⊗] Abstract published in *Advance ACS Abstracts,* July 1, 1996.

S0022-3654(96)00469-8 CCC: $12.00

recombination (time constant τ_{CR}^{II}). The other channel results in free ions by charge separation (τ_{CS}^{II}) with subsequent slow recombination. In general these free ions have lifetimes in the several 100 ns regime.[5,10]

For other donor−acceptor systems[11−13] differences of the complexes CT I and CT II are found by analyzing the charge recombination rates of the two complexes. In addition different dependencies on the free energy ΔG_{CT} of the CT complexes are reported and attributed to varying distances between the donor and acceptor molecules in the formed complexes so that the influence of the surrounding solvent molecules is changed.[14] In this paper the dynamics and optical quantities of all involved states are determined in the case of the DAC or donor excitation.

To investigate these quantities, two different techniques are applied: (a) the common pump−probe measurement is used to determine the transient absorption in a certain wavelength range together with related time constants; (b) degenerate four-wave mixing (DFWM) serves as a probing method in combination with optical pumping of the sample.[7,15,16] The transient changes of the nonlinear susceptibility $\chi^{(3)}$ are studied, yielding the time constants and the molecular hyperpolarizabilities of the molecular states populated in the course of our measurement.

2. Experimental Section

Picosecond light pulses (20 ps, 20 mJ) at a frequency of 9398 cm^{-1} are generated in an actively/passively mode-locked Nd:YAG laser. Two additional intense light pulses are produced at 18797 cm^{-1} by frequency doubling in a KDP crystal and at 28193 cm^{-1} by the two-step generation of the third harmonic in two KDP crystals.[17] The following measurements are performed.

(a) Pump and probe experiments investigate the transient absorption after excitation at 18 797 cm^{-1} or, alternatively, at 28 193 cm^{-1}. We work at moderate pump intensities of a few 10^7 W/cm^2. The change of the sample transmission during the photochemical reaction is monitored by weak probing pulses of variable time delay at the three frequency positions mentioned above. A magic polarization geometry is applied so that reorientational motion does not effect the measured signal transients.

Transient absorption spectra between 14 000 and 22 000 cm^{-1} are measured by the help of a picosecond continuum. The latter is generated focusing part of the second harmonic of the laser output into a cell of 5 cm length containing water.[18] Well-defined small-frequency components are selected from the continuum by a tunable interference filter and used as probing pulses at various spectral positions.

(b) Degenerate four-wave mixing (DFWM) in the self-diffraction geometry is applied as a probing process in the experimental configurations described previously.[7,15,16] In short, two input pulses of equal intensity I_1 (vertically polarized) are temporally and spatially overlapped in the sample cuvette, 500 μm in length. The interaction of the two coherent laser beams with the nonlinear medium over a width of approximately 150 μm results in a transient polarization grating.[19] The diffraction efficiency of the grating η_M in first order is the observed quantity, defined by $\eta_M = I_D/I_1$, where I_D is the diffracted light intensity. The input intensity I_1 ranges between 1 and 10 MW/cm^2 depending on the magnitude of the nonlinear susceptibility $\chi^{(3)}$ that describes the DFWM process. The relation between η_M, the nonlinear susceptibility $\chi^{(3)}(-\omega,\omega,-\omega,\omega)$, and the input pulse intensity I_1 may be written as follows:[19,20]

$$\eta_M = \left(\frac{\omega}{2\epsilon_0 c^2 n^2}\right)^2 |\chi^{(3)}|^2 \left(\frac{1-\exp(-\alpha d)}{\alpha \exp(\alpha d/2)}\right)^2 {I_1}^2 \qquad (1)$$

Here we introduce the following abbreviations: vacuum light velocity c, refractive index n, interaction length d, and absorption coefficient α of the sample at the frequency ω. The unknown susceptibility $|\chi^{(3)}(-\omega,\omega,-\omega,\omega)|$ at different frequencies can be determined by measuring η_M.

The dynamics of the molecular system is studied by DFWM in combination with the optical excitation of the sample.[15,16] To this end, an intense pump pulse−at 18797 or 28193 cm^{-1}−excites a certain amount of the molecules within the volume probed by DFWM. The resulting changes of the diffraction efficiency due to the subsequent photophysical and photochemical processes are observed as a function of delay time t_D.

The investigated samples are solutions of commercially available pyrene and pyromelitic dianhydride (Aldrich) in spectrograde tetrahydrofurane, which has a relatively small polarity ($\epsilon = 7.6$). The pyrene concentration is varied between 0.01 and 0.02 M, whereas the PMDA concentration ranges between 0 and 0.5 M. All measurements are performed at room temperature.

3. Results

Three subjects are investigated by transient absorption measurements and by degenerate four-wave mixing experiments: (i) the ground state of the donor−acceptor complex (DAC); (ii) the dynamics of the DAC following the excitation with pump pulses at 18 797 cm^{-1}; and (iii) the dynamics of the solution when predominantly pyrene is excited at 28 193 cm^{-1}.

(i) The Ground State Donor−Acceptor Complex (DAC). The stationary absorption spectra of pyrene (dashed line) and of PMDA (solid line) dissolved in THF are depicted in Figure 1 together with a binary solution of pyrene/PMDA (dotted line). The latter solution shows a drastic change of the absorption compared to the sum of the spectra of the pure pyrene and PMDA solutions: Besides the increase of the low-frequency tail of the ground state absorption, a new broad absorption appears peaked at 21 600 cm^{-1}. This band is characteristic of a ground state donor−acceptor complex previously observed in the solvent acetonitrile.[5] The molar extinction coefficient of the DAC peak is determined by measuring the absorption coefficient of a series of pyrene/PMDA solutions at 21 600 cm^{-1} with a fixed pyrene concentration of 0.01 M, while the PMDA concentration is varied between 0 and 0.5 M. A Bensi−Hildebrand plot[8] provides the molar extinction coefficient of the DAC at 21 600 cm^{-1} of $\epsilon_{DAC} = 520 \pm 300$ M^{-1} cm^{-1}. Additional measurements suggest that even at the highest PMDA concentrati on of 0.5 M only part of the pyrene molecules form ground state donor−acceptor complexes (DACs). For the binary solution of Figure 1 with $c_{Py} = 0.01$ M and $c_{PMDA} = 0.5$ M the concentration of the DACs amounts to approximately 4×10^{-3} M; that is, only 40% of the pyrene molecules form a ground state DAC.

DFWM experiments without excitation are performed with pure pyrene and pure PMDA solutions as well as pyrene/PMDA mixtures at the three frequencies mentioned above. In solutions the macroscopic susceptibility $\chi^{(3)}$ is made up by a solvent contribution and the molecular hyperpolarizabilities $\gamma_{i,j}^{(3)}$ of the solute molecules i in their respective states j. For noninteracting particles we may write[22]

$$\chi^{(3)} = \chi^{(3)}_{THF} + \frac{N_A L^{(4)}}{\epsilon_0} \sum_{i,j} c_{i,j}(t) \gamma^{(3)}_{i,j} \qquad (2)$$

Here $\chi^{(3)}_{THF}$ denotes the nonlinear susceptibility of the solvent THF; N_A Avogadro's number, $L^{(4)}$ a Lorentz correction factor for the local electric field;[21] and $c_{i,j}(t)$ the concentration of the molecule i in its energy level j at time t. It should be noted that the hyperpolarizabilities $\gamma^{(3)}_{i,j}$ represent orientational averages. Measuring $\chi^{(3)}$ of the pure solutions as a function of the solute concentration (c_{Py} and c_{PMDA}, respectively) allows the determination of the magnitude and the phase of the complex quantity $\gamma^{(3)} = |\gamma^{(3)}|e^{i\phi}$. The measured $\gamma^{(3)}$ values of the ground state pyrene and PMDA are summarized in Table 1 for the three probing frequencies $\omega/2\pi c$. The nonlinear susceptibility of the solvent THF is determined to be $\chi^{(3)}_{THF} = 1.5 \times 10^{-22}$ m^2/V^2 independent of frequency. This value agrees well with literature data.[23] The corresponding molecular hyperpolarizability is estimated to be $\gamma^{(3)}_{THF} = 4.5 \times 10^{-62}$ A s m^4 V^{-3}. It is this small value that makes THF a highly favorable solvent for DFWM experiments. We turn to the determination of nonlinear susceptibility of DAC. In Figure 2 the experimental $|\chi^{(3)}|$ values of pyrene/PMDA mixtures ($c_{Py} = 0.01$ M) are plotted as solid circles versus the PMDA concentration for a DFWM frequency of 18 797 cm^{-1}. For a comparison the calculated sum of the pure pyrene and PMDA solutions is also shown (broken line), representing a fictitious uncomplexed mixture. The solute contribution is indicated by the dotted horizontal line. The difference between the broken line and the data points (i.e. straight line) in Figure 2 provides evidence for the formation of the DAC. From the measured excess amount of $\chi^{(3)}$ the nonlinear hyperpolarizability $\gamma^{(3)}_{DAC}$ of the ground state DAC is determined. Equivalent measurements at the two other frequencies (9398 and 28 193 cm^{-1}) show qualitatively the same behavior. The deduced molecular hyperpolarizabilities of the DAC are listed in Table 2.

TABLE 1: Molar Extinction Coefficient ϵ and Molecular Hyperpolarizability $\gamma^{(3)}$ for the Pyrene S_0 and PMDA S_0 States at the Frequencies 9398, 18797, and 28193 cm^{-1}

	pyrene S_0			PMDA S_0		
frequency (cm^{-1})	ϵ (M^{-1} cm^{-1})	$\lvert\gamma^{(3)}\rvert$ (A s m^4 V^{-3})	φ (deg)	ϵ (M^{-1} cm^{-1})	$\lvert\gamma^{(3)}\rvert$ (A s m^4 V^{-3})	φ (deg)
9398	<1	1.0×10^{-59}	0	<1	1.3×10^{-60}	0
18 797	<1	1.5×10^{-59}	0	<1	1.4×10^{-60}	0
28 193	360	1.4×10^{-57}		<1	1.2×10^{-60}	0

(ii) Excitation of the DAC. With an intense pump pulse at 18 797 cm^{-1} only the DAC in the binary solution is excited (see left arrow in Figure 1), since pyrene and PMDA molecules themselves do not show absorption at this frequency. The time evolution of the transient absorption after excitation is depicted in Figure 3 for a pyrene/PMDA solution with $c_{Py} = 0.02$ M and $c_{PMDA} = 0.5$ M. Approximately 25% of the DAC are excited by the pump pulse. A rapid increase of the absorption within the time resolution of the apparatus (≈10 ps) is observed during the excitation around $t = 0$ ps. The time constant of the following decay is determined to be $\tau_I = 35 \pm 5$ ps, in satisfactory accordance with a published value.[5] The signal transient presents evidence for the formation of a charge transfer complex termed CT I. At long delay times the absorbance approaches the initial value prior to excitation; that is, charge separation leading to long-lived ions is of minor importance. At the probe frequencies of 9398 and 28 193 cm^{-1} one finds different values of $\Delta\alpha$, but the transient absorption recovers with the same time constant $\tau_I = 35$ *ps*, representing the lifetime of CT I. Taking into account the degree of excitation, the $\Delta\alpha$ values allow the evaluation of the molar absorption constant ϵ of CT I (see Table 2).

TABLE 2: Molar Extinction Coefficient ϵ and Molecular Hyperpolarizability $\gamma^{(3)}$ for the Ground State DAC and the CT I Complex at the Frequencies 9398, 18797, and 28193 cm^{-1}

	DAC			CT I		
frequency (cm^{-1})	ϵ (M^{-1} cm^{-1})	$\lvert\gamma^{(3)}\rvert$ (A s m^4 V^{-3})	φ (deg)	ϵ (M^{-1} cm^{-1})	$\lvert\gamma^{(3)}\rvert$ (A s m^4 V^{-3})	φ (deg)
9398	<1	2.2×10^{-59}	0	120	2.5×10^{-58}	180
18 797	170	2.1×10^{-58}	0	870	8.3×10^{-58}	115
28 193	2200	5.4×10^{-57}	0	6000	1.0×10^{-56}	180

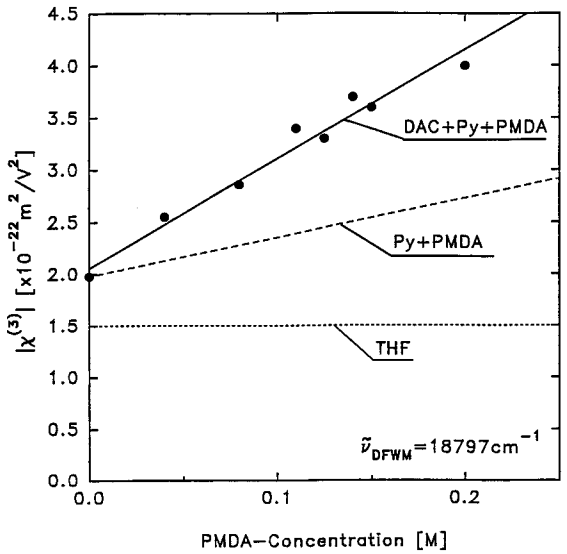

Figure 2. Nonlinear susceptibility $|\chi^{(3)}|$ at 18 797 cm^{-1} versus PMDA concentration for constant $c_{Py} = 0.01$ M (experimental points). Dotted line: $\chi^{(3)}$ of the pure solvent THF. Broken line: sum of $\chi^{(3)}$ of pyrene and PMDA. Solid line through experimental points: observed $\chi^{(3)}$ of pyrene and PMDA solution indicating the DAC contribution.

Additional information on the charge transfer complex is obtained from the transient spectrum of the sample investigated in the range from 14 000 to 22 000 cm^{-1}. The spectrum measured 10 ps after excitation is depicted in the inset of Figure 3. It provides direct evidence for charge separation. The strong absorption band, located at 22 200 cm^{-1}, coincides with an electronic transition of Py^+. The second maximum at 15 900 cm^{-1} corresponds to an absorption band of $PMDA^-$.[6]

We now turn to a discussion of the DFWM probing. The time evolution of the diffraction efficiency η_M after pumping of the DAC at 18 797 cm^{-1} is studied at the same three frequencies as the transient absorption. In Figure 4 experimental data are presented for $\omega/2\pi c = 9398$ cm^{-1}. One sees a drastic change of η_M with excitation. Similar to the transient absorption experiment, the DFWM shows a rapid change of η_M around $t_D = 0$ ps and a subsequent return to the initial value according to $\exp(-2t/\tau_I)$. The factor of 2 originates from the quadratic number density dependence of the DFWM signal. A lifetime of $\tau_I \simeq 35$ ps is again measured, indicating that the same dynamics is observed as in the probe absorption. During the excitation the diffraction efficiency decreases from $\eta_M = 2.5 \times 10^{-4}$ to 1.5×10^{-4}. This strong decrease of η_M cannot be explained by a depletion of the ground state of the DAC. The latter contributes only 20% to the total signal ($t_D < -10$ ps) and only 10% of the DAC are excited. A new species, CT I, is formed with considerably larger nonlinearity. To account for the reduced scattering efficiency, the CT I complex at $\tilde{\nu}_{DFWM}$

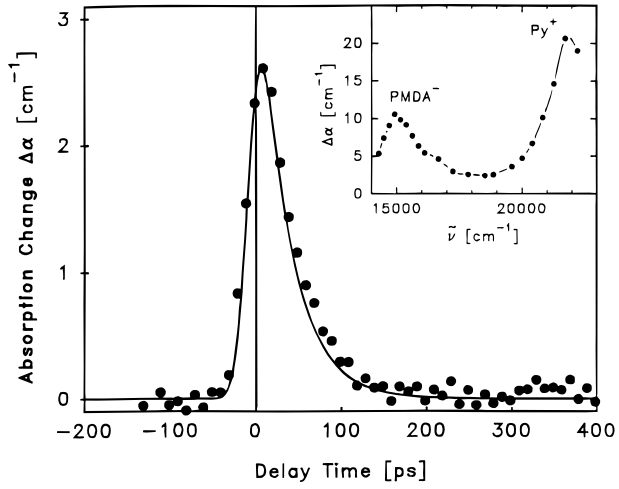

Figure 3. Transient change of the absorption coefficient $\Delta\alpha$ versus delay time between excitation pulse at 18 797 cm^{-1} and a probe pulse at the same frequency, experimental points. Concentrations of pyrene and PMDA are 0.02 and 0.5 M, respectively; approximately 15% of the ground state DAC are excited. Calculated solid line for monoexponential decay of CT I with a time constant of 35 ps. Inset: the transient absorption spectrum in the frequency range 14 000-23 000 cm^{-1} measured at $t_D = 10$ ps; the peaks at 22 200 and 15 900 cm^{-1} correspond to absorption bands of the pyrene cation and the PMDA anion, respectively.

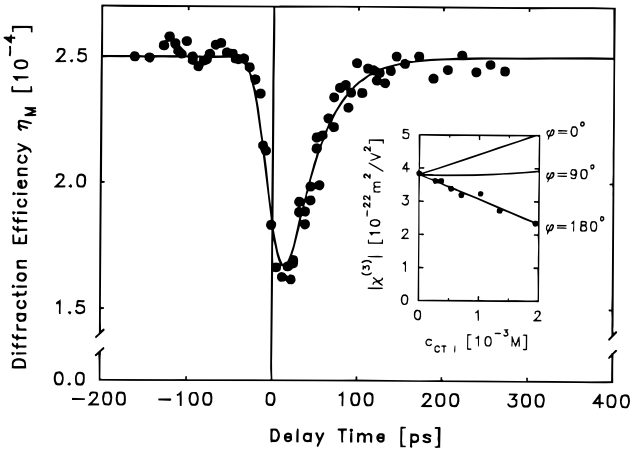

Figure 4. Time-resolved diffraction efficiency η_M versus delay time for DFWM probing after excitation of 25% of the ground state DAC at 18 797 cm^{-1}. The probe frequency of the two input pulses generating the transient grating is 9398 cm^{-1}; concentrations $c_{Py} = 0.02$ M and $c_{PMDA} = 0.5$ M: experimental points; calculated solid line. Inset: nonlinear susceptibility $|\chi^{(3)}|$ for $t_D = 10$ ps versus the concentration of the CT I complex (excitation at 18 797 cm^{-1}). The strong decrease of the data points indicates a negative sign of $\gamma^{(3)}$ of CT I; calculated solid lines for different phase parameters φ.

$= 9398$ cm^{-1} has to display an opposite sign of $\gamma^{(3)}$ as compared to that of the ground state DAC. To corroborate this result, the DFWM experiment was performed with increasing excitation of the DAC, varying the pump intensity. The inset of Figure 4 shows $|\chi^{(3)}|$ deduced from the diffraction efficiency as a function of the resulting concentration of the CT I complex. The data are taken 10 ps after the peak of the pump pulse. The solid line fitted to the data points yields the magnitude as well as the phase of $\gamma^{(3)}_{CTI}$. The negative sign corresponds to $\varphi = 180°$. The time dependency of η_M and the magnitude of $\gamma^{(3)}_{CTI}$ at the two other frequencies 18 797 and 28 193 cm^{-1} show qualitatively the same behavior. The obtained values of $\gamma^{(3)}$ for CT I are summarized in Table 2.

(iii) Excitation of Pyrene. The dynamics of the electron transfer after excitation of the pyrene molecule with pump pulses

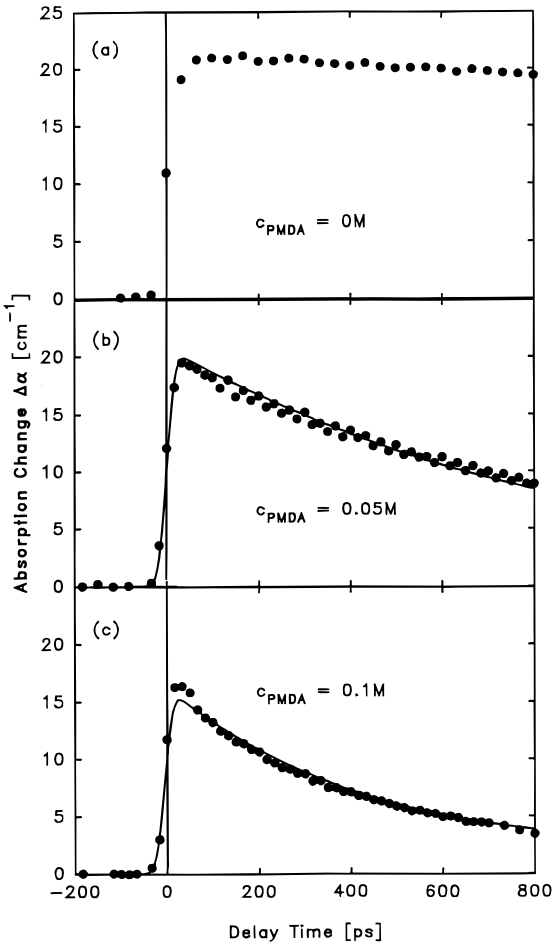

Figure 5. Transient absorption change of pyrene/PMDA in THF versus delay time at a probe frequency of 28 193 cm^{-1} after excitation at 28 193 cm^{-1} (concentrations $c_{Py} = 0.02$ M and $c_{PMDA} = 0$ M (a), 0.05 M (b), and 0.1 M (c)). Approximately 6% of the pyrene molecules are excited; experimental points; calculated solid lines.

at 28 193 cm^{-1} is studied in the following. At this pump frequency the DAC also shows some absorption, as seen in Figure 1. To minimize the contribution of the DAC excitation, the PMDA concentration—and correspondingly the DAC concentration—is notably decreased in comparison to the previous subsection. All measurements are performed at a fixed pyrene concentration of $c_{Py} = 0.01$ M and at three different PMDA concentrations, $c_{PMDA} = 0$, 0.05, and 0.1 M. For $c_{PMDA} = 0.05$ M 7 times more pyrene molecules are excited than DACs. The short lifetime of CT I of 35 ps is also helpful to minimize its possible contribution to the signal transients for $t_D > 50$ ps. Figure 5 shows the time evolution of the absorption changes at equal pump and probe frequencies of 28 193 cm^{-1}. Approximately 6% of the pyrene molecules are excited by the pump pulse. In pure pyrene solutions (Figure 5a) the absorption increases rapidly around $t_D = 0$ ps within the time resolution of the apparatus and decays slowly for later delay times. This transient absorption is due to the larger ϵ value of the excited Py S_1 state (compare Tables 1 and 3 for Py S_0 and Py S_1). The time behavior is in agreement with the long lifetime of the pyrene S_1 state ranging between 300 and 475 ns in various solvents.[8] Quite different is the time dependence of $\Delta\alpha$ after adding PMDA to the pyrene solution. For $c_{PMDA} = 0.05$ M (Figure 5b) and 0.1 M (Figure 5c) the absorption at later delay times, >50 ps, shows a clear dependence on the PMDA concentration. An increase of the PMDA number density results in a decrease of the initial $\Delta\alpha$ value and a faster subsequent decay. At the two other probe frequencies, 9398 and 18 797

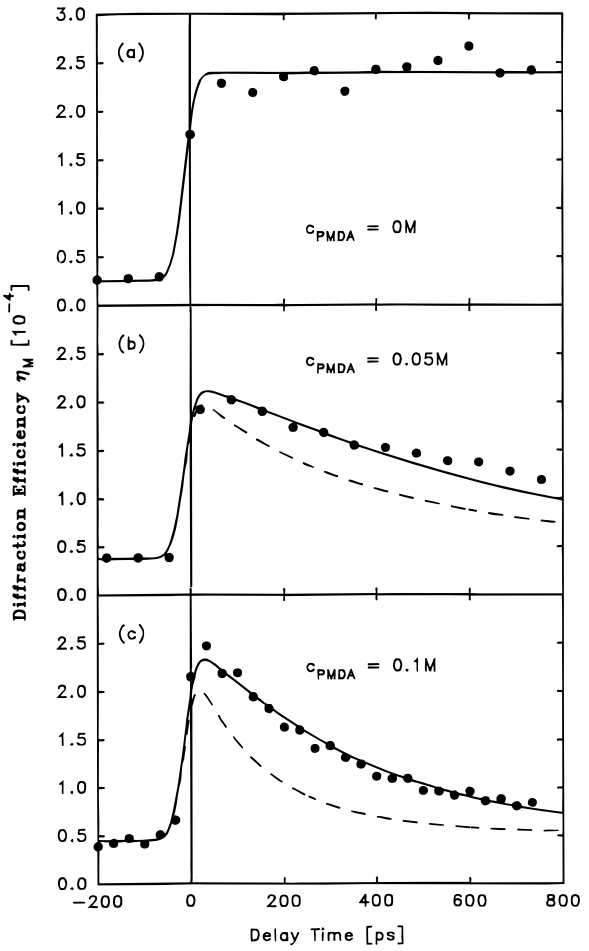

Figure 6. Efficiency η_M versus delay time for different pyrene/PMDA solutions: $c_{pyrene} = 0.02$ M, $c_{PMDA} = 0$ M (a), 0.05 M (b), and 0.1 M (c); excitation at 28 193 cm^{-1} and DFWM probing at 9398 cm^{-1}. Experimental points, calculated solid line. The dashed curves are obtained from the same model calculation by replacing the $\gamma^{(3)}$ value of CT II by that of CT I.

TABLE 3: Molar Extinction Coefficient ϵ and Molecular Hyperpolarizability $\gamma^{(3)}$ for the Pyrene S_1 State and the CT II Complex at the Frequencies 9398, 18797, and 28193 cm^{-1}

	pyrene S_1			CT II		
frequency (cm^{-1})	ϵ (M^{-1} cm^{-1})	$\lvert\gamma^{(3)}\rvert$ (A s m^4 V^{-3})	φ (deg)	ϵ (M^{-1} cm^{-1})	$\lvert\gamma^{(3)}\rvert$ (A s m^4 V^{-3})	φ (deg)
9398	300	1.5×10^{-57}	0	190	2×10^{-57}	0
18 797	800	1.8×10^{-58}	0	400	4×10^{-58}	180
28 193	8200	8.3×10^{-57}	180	2900	$<1.5 \times 10^{-57}$	

cm^{-1}, a similar behavior is observed. The ϵ values of CT II deduced from the observed $\Delta\alpha$ values and the applied pump intensities are listed in Table 3. The solid curves through the experimental data points in Figure 5 are calculated considering the relaxation scheme II depicted in the Introduction and the time constants discussed below. We note that the relaxation scheme II introduces a charge transfer complex CT II. It will be shown below that CT II differs from CT I.

The time evolution of the diffraction efficiency η_M of DFWM probing is studied at the same three frequencies as for the transient absorption measurements. Figure 6 presents the time evolution of η_M for different PMDA concentrations at $\tilde{\nu}_{DFWM} = 9398$ cm^{-1}. Approximately 4% of the pyrene molecules are excited at 28 193 cm^{-1} at the chosen pump intensity. The pure pyrene solution (Figure 6a) shows—similar to the transient absorption measurement—a rapid change of η_M within the duration of the excitation pulse at $t = 0$ ps. The subsequent high level of η_M during the observed time interval indicates a large hyperpolarizability of pyrene in the S_1 state. The dynamics of η_M changes substantially when PMDA is added to the pyrene solution (Figure 6b,c). Here one finds a decrease of the diffraction efficiency, which shows again a distinct PMDA concentration dependence; that is, $|\chi^{(3)}|$ decreases more rapidly by the formation and subsequent relaxation of CT II. The transient η_M at 18 797 and 28 193 cm^{-1} exhibits similar time dependencies. The solid lines through the experimental points and the broken line of Figure 6 are calculated as discussed below. The $\gamma^{(3)}$ values of CT II are listed in Table 3.

4. Discussion

Following the subtitles of the preceeding section, we wish to discuss (i) the data on the ground states of the pyrene and PMDA molecules as well as of the donor−acceptor complex DAC; (ii) the observation of the charge transfer complex CT I derived from DAC by direct excitation at 18 797 cm^{-1}; (iii) evidence for a charge transfer complex CT II after excitation of pyrene; and (iv) a comparison between the charge transfer complexes CT I and CT II.

At the beginning, a comment should be made on the magnitude of the measured molecular hyperpolarizability $\gamma^{(3)}$. Theory predicts that $\gamma^{(3)}$ consists of 24 terms,[24] four of which display one-photon resonances. As a consequence $\gamma^{(3)}$ is resonantly enlarged in the frequency range of strong absorption. Far from optical resonances, $|\gamma^{(3)}|$ is small due to the nonresonant terms with little frequency dependence.

(i) The molar extinction coefficients derived from the stationary absorption spectra for pyrene S_0, PMDA S_0, and DAC in the electronic ground state (Figure 1) are listed for three frequencies in Tables 1 and 2. The ϵ values are small in general; only at 28 193 cm^{-1} do DAC and pyrene give evidence of near resonances. As expected, the $\gamma^{(3)}$ values are small for the lower frequencies, but at 28 193 cm^{-1} substantially larger numbers are measured. It is noteworthy that $|\gamma^{(3)}|$ of DAC exceeds the sum of the pyrene and PMDA values by a factor of approximately 4.

(ii) The excitation of the ground state DAC leads to the rapid appearance of two transient absorption bands (see inset of Figure 3), similar to the spectra of the cation of pyrene and the anion of PMDA. This observation suggests the transfer of one full charge between pyrene and PMDA. According to the reaction scheme I, the generated charge transfer complex is called CT I. The time scale of the process is short compared to the experimental pulse duration. In Figure 3 a maximum change of absorption $\Delta\alpha = 2.7$ cm^{-1} is observed for an excitation of 15% of the DAC concentration. These numbers give a molar extinction coefficient $\epsilon_{CTI} = 870$ M^{-1} cm^{-1} at 18 797 cm^{-1} (see Table 2). The transient absorption of Figure 3 decays with a single-exponential time constant of $\tau_I = 35 \pm 5$ ps. There is no evidence of a residual absorption for long delay times, which might suggest some dissociated (long-lived) free ions. We conclude that the observed time constant represents the fast charge recombination time τ_{CR}^{I} by which the complex CT I returns to DAC. Additional information on the formation of the CT I complex comes from the DFWM experiments of Figure 4. The rapid change of the diffraction efficiency η_M around $t_D = 0$ ps and the return of η_M or correspondingly $|\chi^{(3)}|$ to the initial value with a time constant of $\tau_I = 35$ ps support the dynamics of the short-lived CT I complex as seen in the transient absorption studies (Figure 3). According to Table 2, the values of ϵ and $|\gamma^{(3)}|$ increasing with frequency display a similar resonance behavior. The negative value of $\gamma^{(3)}$ is physically possible but not well understood at the present time. Of interest

is a comparison of the ϵ and $|\gamma^{(3)}|$ values of the two complexes DAC and CT I. Both values are larger for CT I than for DAC at the three investigated frequencies. The substantial differences of the ϵ and $|\gamma^{(3)}|$ data allow a ready distinction of the two complexes and enables us to study the dynamics of CT I.

(iii) The direct excitation of the pyrene molecules with pulses at 28 193 cm^{-1} leads to the population of the long-lived pyrene S_1 state. Subsequent encounter of the excited pyrene with a ground state PMDA molecule generates the charge transfer complex CT II made up of pyrene$^+$- and PMDA$^-$-like constituents.[6] Charge recombination to the ground state molecules and dissociation to free ions govern the lifetime of CT II. We have performed model calculations based on rate equations according to the reaction scheme II. The results are compared with the transient data of Figures 5 and 6 and the similar results for the two additional probe frequencies. The following assumptions are made: The molar extinction coefficients of CT II and of the free cation and anion pairs are taken to be approximately the same;[2,25] the charge transfer rate $1/\tau_{CT}$ depends linearly on PMDA concentration.[8] The latter assumption is justified since the chemical process is diffusion controlled in the present solution. The transient absorption data at three probe frequencies and at two different concentrations of PMDA are analyzed. Four molecular states are relevant: The ground state S_0 and the excited state S_1 of pyrene, the charge transfer complex CT II, and the separated ions. A theoretical estimate of τ_{CT} is possible via eq 3:[8]

$$\frac{1}{\tau_{CT}} = \frac{8RT}{3000\eta}\left(\frac{pa}{b}\right)[\mathrm{M}^{-1}\,\mathrm{cm}^{-1}] \qquad (3)$$

Here T denotes the temperature; η the viscosity of the solvent THF ($\eta = 0.49$ cP); a an interaction radius; b the Stokes radius; and p the probability of a reaction per collision. With the factor (pa/b) close to 1, a reasonable value for various charge transfer systems,[8] one estimates the value of $\tau_{CT} = 37$ ps M/c_{PMDA}. A somewhat larger number is suggested by the theory of ref 26 depending on the free energy change ΔG of the charge transfer reaction. Unfortunately, the latter quantity is not accurately known for the present system.

The model calculations are fitted to our extensive body of data providing the important time constants and ϵ values. τ_{CT} for the buildup of CT II is found to be $\tau_{CT} = 25$ ps M/c_{PMDA}, in fair agreement with the theoretical value mentioned above. With the time constants $\tau_{CR}^{II} = 400$ ps and $\tau_{CS}^{II} = 1$ ns, together with the ϵ values of Table 3, the experimental absorption data are well accounted for (e.g. solid lines through experimental points in Figure 5). In Figure 7 the computed concentrations of the four molecular states (Py S_0, Py S_1, CT II, and the ions) are plotted versus time. Figure 7 illustrates the reaction scheme II, in particular the formation of the charge transfer complex CT II starting from the excited Py S_1 state and the influence of the reaction partner PMDA on this process.

With the help of the concentration data of Figure 7 it is straightforward to determine the $\gamma^{(3)}$ values of the Py S_1 and the CT II species using the experimental data of the diffraction efficiency (see computed solid lines in Figure 6). The obtained values for $|\gamma^{(3)}|$ and the phases are listed in Table 3.

(iv) The different time evolution of the probe absorption data (compare Figures 3 and 5) suggests that two different complexes, CT I and CT II, are generated at the two excitation frequencies of 18 797 and 28 193 cm^{-1}. Some support to this point is given by the different ϵ values of Tables 2 and 3 for the two complexes. Convincing evidence is obtained from the DFWM investigations. We point to the drastic differences of η_M in magnitude and time dependence for the two excitation frequencies (compare Figures 4 and 6). The different sign of $\gamma^{(3)}$ at 9398 cm^{-1} is particularly significant in this respect. The data give clear evidence for the different character of the charge transfer complexes CT I and CT II with charge recombination times of 35 and 400 ps, respectively.

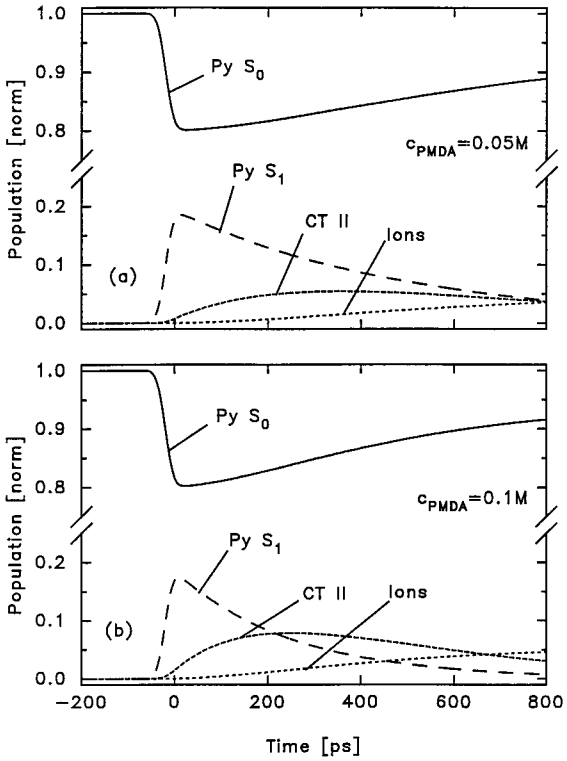

Figure 7. Calculated populations of the relevant molecular states (in normalized units) after excitation of a pyrene/PMDA solution in THF at 28 193 cm^{-1}. Different PMDA concentrations: $c_{PMDA} = 0.05$ M (a) and $c_{PMDA} = 0.1$ M (b); $c_{Py} = 0.02$ M.

Unfortunately, information on the potential surfaces and structural differences of the two species is not available at the present time. We note in this context that two excited charge transfer complexes were recently predicted for the system benzene/tetracyanoethylene (in addition to the ground state complex) with different relative positions of the donor and acceptor molecules, different binding energies, and a separation of the corresponding minima of the potential surfaces of several hundred cm^{-1}.[27] A similar situation may be surmised for pyrene/PMDA; it is not unreasonable in this picture that the different excitation processes via the electronically excited DAC* or the pyrene S_1 state lead to different potential surfaces and minimum positions.

References and Notes

(1) Hubig, S. M. *J. Phys. Chem.* **1992**, *96*, 2903.
(2) Goodman, J. L.; Peters, K. S. *J. Am. Chem. Soc.* **1985**, *107*, 6459.
(3) Goodman, J. L.; Peters, K. S. *J. Am. Chem. Soc.* **1985**, *107*, 1441.
(4) Mataga, N.; Kanda, Y.; Asahi, T.; Miyasaka, H.; Okada, T. *Chem. Phys.* **1988**, *127*, 239.
(5) Mataga, N.; Shioyama, H.; Kanda Y. *J. Phys. Chem.* **1987**, *91*, 314.
(6) Asahi, T.; Mataga, N. *J. Phys. Chem.* **1991**, *95*, 1956.
(7) Assel, M.; Höfer, T.; Laubereau, A.; Kaiser, W. *Chem. Phys. Lett.* **1995**, *234*, 151.
(8) Birks, J. B. *Photophysics of Aromatic Molecules*; J. Wiley & Sons Ltd.: New York, 1970.
(9) Kavarnos, G. J. *Fundamentals of Photoinduced Electron Transfer*; VCH Publishers Inc.: Weinheim, 1993.
(10) Hirata, Y.; Kanda, Y.; Mataga, N. *J. Phys. Chem.* **1983**, *87*, 1659.
(11) Asahi, T.; Mataga, N. *J. Phys. Chem.* **1989**, *93*, 6575.
(12) Ojima, S.; Miyasaka, H.; Mataga, N. *J. Phys. Chem.* **1990**, *94*, 7534.
(13) Miyasaka, H.; Nagata, T.; Kiri, M.; Mataga, N. *J. Phys. Chem.* **1992**, *96*, 8060.

(14) Kakitani, T.; Mataga, N. *J. Phys. Chem*. **1986**, *90*, 993.
(15) Höfer, T.; Kruck, P.; Kaiser, W. *Chem. Phys. Lett.* **1994**, *224*, 411.
(16) Höfer, T.; Kruck, P.; Elsaesser, T.; Kaiser, W. *J. Phys. Chem*. **1995**, *99*, 4380.
(17) Craxton, R. S. *IEEE J. Quantum Electron* **1981**, *QE-17*, 177.
(18) Penzkofer, A.; Laubereau, A.; Kaiser, W. *Phys. Rev. Lett.* **1973**, *31*, 863.
(19) Eichler, H.; Günter, P.; Pohl, D. W. *Laser-Induced Dynamic Gratings*; Springer-Verlag: Berlin, Heidelberg, 1986.
(20) Langhans, D.; Salk, J.; Wiese, W. *Physica* **1987**, *144c*, 411.
(21) Boyd, J. B.; Dyson, D. J. *Proc. R. Soc. A* **1963**, *275*, 135.
(22) Leupacher, W.; Penzkofer, A. *Appl. Phys. B* **1985**, *36*, 25.
(23) Prasad, P. N.; Wiliams, D. J. *Introduction to Nonlinear Effects in Molecules and Polymers*; Wiley: New York, 1991.
(24) Flytzanis, C. *In Quantum Electronics*; Rabin, H., Lang, C. L., Eds.; Academic Press: New York, 1975; p 9.
(25) Mataga, N.; Asahi, T.; Kanda, Y.; Okada, T. *J. Phys. Chem*. **1987**, *91*, 249.
(26) Tachiya, M.; Murata, S. *J. Phys. Chem*. **1992**, *96*, 8441.
(27) Emery, L. C.; Sheldon, J. M.; Edwards, W. D.; McHale, J. L. *Spectrochim. Acta* **1992**, *48A*, 715.

JP960469+